A new strategy for label-free detection of lymphoma cancer cells

Nicola M. Martucci,[1,*] Ilaria Rea,[2] Immacolata Ruggiero,[1] Monica Terracciano,[2,3] Luca De Stefano,[2] Nunzia Migliaccio,[1] Camillo Palmieri,[4] Giuseppe Scala,[4] Paolo Arcari,[1] Ivo Rendina,[2] and Annalisa Lamberti[1]

[1]*Department of Molecular Medicine and Medical Biotechnology, University of Naples Federico II, Via S. Pansini 5, 80131 Naples, Italy*
[2]*Institute for Microelectronics and Microsystems, National Council of Research, Via P. Castellino 111, 80131 Naples, Italy*
[3]*Department of Pharmacy, University of Naples Federico II, Via Domenico Montesano 49, 80131 Naples, Italy*
[4]*Department of Experimental and Clinical Medicine, University "Magna Graecia" of Catanzaro, Viale Europa, 88100 Germaneto, Catanzaro, Italy*
[*]*nicolamassimiliano.martucci@unina.it*

Abstract: In this paper, a new strategy for highly selective and sensitive direct detection of lymphoma cells by exploiting the interaction between a peptide and its B-cell receptor, has been evaluated. In particular, an idiotype peptide, able to specifically bind the B-cell receptor of A20 cells in mice engrafted with A20 lymphoma, has been used as molecular probe. The new detection technique has been demonstrated on a planar crystalline silicon chip. Coverage of 85% of silicon surface and detection efficiency of 8.5×10^{-3} cells/μm^2 were obtained. The recognition strategy promises to extend its application in studying the interaction between ligands and their cell-surface receptors.

OCIS codes: (000.1430) Biology and medicine; (280.1415) Biological sensing and sensors.

References and links

1. K. Brindle, "New approaches for imaging tumour responses to treatment," Nat. Rev. Cancer **8**(2), 94–107 (2008).
2. L. Fass, "Imaging and cancer: a review," Mol. Oncol. **2**(2), 115–152 (2008).
3. T. Mosmann, "Rapid colorimetric assay for cellular growth and survival: application to proliferation and cytotoxicity assays," J. Immunol. Methods **65**(1-2), 55–63 (1983).
4. J. Zhang, R. E. Campbell, A. Y. Ting, and R. Y. Tsien, "Creating new fluorescent probes for cell biology," Nat. Rev. Mol. Cell Biol. **3**(12), 906–918 (2002).
5. R. de la Rica, S. Thompson, A. Baldi, C. Fernandez-Sanchez, C. M. Drain, and H. Matsui, "Label-free cancer cell detection with impedimetric transducers," Anal. Chem. **81**(24), 10167–10171 (2009).
6. M. Perfézou, A. Turner, and A. Merkoçi, "Cancer detection using nanoparticle-based sensors," Chem. Soc. Rev. **41**(7), 2606–2622 (2012).
7. J. C. Ehrhart, B. Bennetau, L. Renaud, J. P. Madrange, L. Thomas, J. Morisot, A. Brosseau, S. Allano, P. Tauc, and P. L. Tran, "A new immunosensor for breast cancer cell detection using antibody-coated long alkylsilane self-assembled monolayers in a parallel plate flow chamber," Biosens. Bioelectron. **24**(3), 467–474 (2008).
8. A. Lamberti, C. Sanges, N. Migliaccio, L. De Stefano, I. Rea, E. Orabona, G. Scala, I. Rendina, and P. Arcari, "Silicon-based technology for ligand-receptor molecular identification," J. At. Mol. Opt. Phys. **2012**, 948390 (2012).
9. S. K. Arya, K. Y. Wang, C. C. Wong, and A. R. Rahman, "Anti-EpCAM modified LC-SPDP monolayer on gold microelectrode based electrochemical biosensor for MCF-7 cells detection," Biosens. Bioelectron. **41**, 446–451 (2013).
10. J. Liu, Y. Qin, D. Li, T. Wang, Y. Liu, J. Wang, and E. Wang, "Highly sensitive and selective detection of cancer cell with a label-free electrochemical cytosensor," Biosens. Bioelectron. **41**, 436–441 (2013).
11. S. Bi, J. Zhang, and S. Zhang, "Ultrasensitive and selective DNA detection based on nicking endonuclease assisted signal amplification and its application in cancer cell detection," Chem. Commun. (Camb.) **46**(30), 5509–5511 (2010).
12. C. Pan, M. Guo, Z. Nie, X. Xiao, and S. Yao, "Aptamer-based electrochemical sensor for label-free recognition and detection of cancer cells," Electroanalysis **21**(11), 1321–1326 (2009).
13. K. Min, K. M. Song, M. Cho, Y. S. Chun, Y. B. Shim, J. K. Ku, and C. Ban, "Simultaneous electrochemical detection of both PSMA (+) and PSMA (-) prostate cancer cells using an RNA/peptide dual-aptamer probe," Chem. Commun. (Camb.) **46**(30), 5566–5568 (2010).

14. Y. Hu, P. Zuo, and B. C. Ye, "Label-free electrochemical impedance spectroscopy biosensor for direct detection of cancer cells based on the interaction between carbohydrate and lectin," Biosens. Bioelectron. **43**, 79–83 (2013).
15. J. Zhao, L. Zhu, C. Guo, T. Gao, X. Zhu, and G. Li, "A new electrochemical method for the detection of cancer cells based on small molecule-linked DNA," Biosens. Bioelectron. **49**, 329–333 (2013).
16. H. Nogai, B. Dörken, and G. Lenz, "Pathogenesis of Non-Hodgkin's Lymphoma," J. Clin. Oncol. **29**(14), 1803–1811 (2011).
17. C. Palmieri, C. Falcone, E. Iaccino, F. M. Tuccillo, M. Gaspari, F. Trimboli, A. De Laurentiis, L. Luberto, M. Pontoriero, A. Pisano, E. Vecchio, O. Fierro, M. R. Panico, M. Larobina, S. Gargiulo, N. Costa, F. Dal Piaz, M. Schiavone, C. Arra, A. Giudice, G. Palma, A. Barbieri, I. Quinto, and G. Scala, "In vivo targeting and growth inhibition of the A20 murine B-cell lymphoma by an idiotype-specific peptide binder," Blood **116**(2), 226–238 (2010).
18. F. De Angelis, A. Pujia, C. Falcone, E. Iaccino, C. Palmieri, C. Liberale, F. Mecarini, P. Candeloro, L. Luberto, A. de Laurentiis, G. Das, G. Scala, and E. Di Fabrizio, "Water soluble nanoporous nanoparticle for in vivo targeted drug delivery and controlled release in B cells tumor context," Nanoscale **2**(10), 2230–2236 (2010).
19. S. Chen, L. Liu, J. Zhou, and S. Jiang, "Controlling Antibody Orientation on Charged Self-Assembled Monolayers," Langmuir **19**(7), 2859–2864 (2003).
20. W. Kern, *Handbook of semiconductor wafer cleaning technology: science, technology, and applications* (William Andrew Publishing/Noyes, 1993).
21. L. A. DeLouise, P. M. Kou, and B. L. Miller, "Cross-correlation of optical microcavity biosensor response with immobilized enzyme activity. Insights into biosensor sensitivity," Anal. Chem. **77**(10), 3222–3230 (2005).
22. L. De Stefano, G. Oliviero, J. Amato, N. Borbone, G. Piccialli, L. Mayol, I. Rendina, M. Terracciano, and I. Rea, "Aminosilane functionalizations of mesoporous oxidized silicon for oligonucleotide synthesis and detection," J. R. Soc. Interface **10**(83), 20130160 (2013).
23. M. Terracciano, I. Rea, J. Politi, and L. De Stefano, "Optical characterization of aminosilane-modified silicon dioxide surface for biosensing," J. Europ. Opt. Soc. Rap. Public **8**, 13075 (2013).
24. K. J. Kim, C. Kanellopoulos-Langevin, R. M. Merwin, D. H. Sachs, and R. Asofsky, "Establishment and characterization of BALB/c lymphoma lines with B cell properties," J. Immunol. **122**(2), 549–554 (1979).
25. I. Rea, G. Oliviero, J. Amato, N. Borbone, G. Piccialli, I. Rendina, and L. De Stefano, "Direct synthesis of oligonucleotides on nanostructured silica multilayers," J. Phys. Chem. C **114**(6), 2617–2621 (2010).
26. J. Kim, P. Seidler, L. S. Wan, and C. Fill, "Formation, structure, and reactivity of amino-terminated organic films on silicon substrates," J. Colloid Interface Sci. **329**(1), 114–119 (2009).

1. Introduction

Cancer is a leading cause of death worldwide. New therapies, including minimal residual disease treatments, crucial for patient survival, seem to strongly depend on the capabilities of detecting cancer cells. Various techniques were developed for cancer cell detection, including cytology test, fluorescent imaging, magnetic resonance imaging, computerized tomography, X-ray radiography and ultrasound [1–4]. However, most of these modalities are highly expensive and time consuming. Moreover, these approaches may be associated to risks deriving from radioactive sources. Therefore, despite some considerable achievements, there still remains a challenge the development of simple, rapid, non-destructive and low cost methods for early detection of cancer and minimal residual disease, important for diagnosis and reduction in mortality for certain cancers [5,6]. Biosensing technology, taking advantage of the properties of biological systems combined to functional advanced materials, is providing rapid, reproducible, and highly sensitive cell detection.

In the last decade, progresses were made to enhance the cell capture on the surface of microchips by antibody-antigen interactions [7–9]. Anyway, the contact probability between cells and antibodies on capture specific surface has still to be improved. Moreover, the existing antibodies are quite limited and their preparation is very complex. In order to overcome these limits, some ligand binding molecules, such as aptamers and lectins, were recently discovered, and more recently, oligonucleotides tethered with target-binding small molecules were considered because the small molecule moiety at the terminal of the oligonucleotides can exhibit reasonable affinity and selectivity towards target molecules [10–15].

In the present work, a new peptide-based strategy to detect lymphoma cells was settled. Lymphomas are cancers that originate from lymphoid cells, which are part of the immune system. B-cell lymphomas arise during different steps of B-lymphocyte development and represent their malignant counterpart [16]. They typically appear with swollen lymph glands, and they can be spread from place of origin to the spleen, liver and bone marrow. The

dissemination of tumor cells can also occur in the blood with a framework similar to that of leukemia. The disease is characterized by an incomplete response to clinical treatment and fatal outcomes. For these reasons, it is imperative to devise new strategies to target specifically the cancer cells that replenish the pool of tumorigenic cells in the course of the minimal residual disease. Surface immunoglobulin (Ig) B-Cell Receptor (IgBCR) is a hallmark of B cells and constitutes an obvious homing moiety for cell specific targeting. Individual B-cell clones differ from one another because of the variable sequences within the antigen-binding site of the expressed IgBCR, which are collectively termed "idiotype" (Id). The Id expressed by lymphoma/leukemic cells is unique for a given clonal population and function as patient-specific tumor antigens that may be exploited for targeted therapies and diagnosis.

The on-chip sensing technique here presented takes advantage of a new functionalization strategy exploiting the Id-peptide as biomolecular probe. The Id-peptides are small peptide ligands able to bind with high affinity and specificity to the Id of lymphoma B cells [17,18]. The use of Id specific peptide as molecular probe could highly improve affinity and selectivity of the capture surface. In addition, it simplifies the biochip functionalization procedure with respect to that employed for antibodies in which controlling protein orientation is still very challenging [19]. In this setting, we constructed an Id-peptide-based biosensor by using as substrate both planar and porous silicon. The comparison between the two materials showed that planar silicon appeared more efficient for the realization of a biosensor for targeting patient-specific neoplastic B cells. This detection strategy could be useful for the development of sensing devices capable of monitoring minimal residual disease.

2. Materials and experimental

2.1. Chemicals and reagents

(3-Aminopropyl)triethoxysilane (APTES), Bis(sulfosuccinimidyl) suberate (BS^3), Dimethyl Sulfoxide (DMSO), Tris(2-carboxyethyl)phosphine hydrochloride (TCEP), Toluene anhydrous and H_2SO_4 were purchased from Sigma-Aldrich (MO, USA). HCl was purchased from Romil (UK). Absolute Ethanol and H_2O_2 were purchased from Carlo Erba (IT), HEPES powder was purchased from Promega (USA). Alexa Fluor 488 C5 maleimide was purchased from Molecular Probes Inc. (OR, USA). Synthesis of both A20-36 and random peptides was performed by CASLO Laboratory (DK).

2.2. Planar and porous silicon chips fabrication

Highly doped p + silicon wafer, <100> oriented, 0.003 Ω·cm resistivity, 400 μm thick, was cut into 10 mm × 10 mm square pieces to obtain planar crystalline silicon (CSi) chips. After cleaning by means of standard RCA process [20], silicon substrates were thermally oxidized at 1050 °C for 5 hours.

Porous crystalline silicon (PSi) has a high specific surface (up to 500 m^2/cm^3), which can be produced by electrochemical etching of planar crystalline silicon. Since the porosity (*i.e.*, the amounts of void in the silicon layer) can be precisely tuned by changing process parameters (such as etching electrical current, acid concentration and so on), the resulting structures can be optically encoded, thus becoming an effective transducer of chemical and biological processes that happen on its surface. For its morphology and low-cost production, PSi is an ideal bulky model system to study surface functionalization of planar silicon, exploiting signal enhancement (*i.e.*, infrared absorption) due to the concentration of chemicals and biological substances in its pores, whereas few nanometers thick layer of passivating agents can be hardly quantified on crystalline silicon surface.

A PSi microcavity constituted by a λ/2 layer (optical thickness) sandwiched between two 9.5 period Bragg reflectors (BRs), was obtained alternating low (L) and high (H) refractive index layers whose thicknesses satisfy the Bragg relationship nHdH + nLdL = mλB/2, where m is an integer and λB is Bragg wavelength. The microcavity was prepared by

electrochemical etching of highly doped p$^+$ planar crystalline silicon (0.001 Ω cm resistivity, <100> oriented, 500 µm thick) in HF solution (HF 50% in weight: ethanol = 1:1) in dark conditions and at room temperature (RT). Before the anodization process, the silicon substrate was immersed in HF solution for 2 min so as to remove the native oxide layer. A current density of 200 mA cm^{-2} for 1.2 s was applied to obtain low refractive index layers (nL = 1.542; dL = 125 nm) while a current density of 100 mA cm^{-2} was applied for 1.4 s for high refractive index layers (nH = 1.784; dH = 108 nm). After electrochemical process, pores dimension was increased so as to favor the infiltration of biological matter by rinsing the fresh-made PSi microcavity in a KOH ethanol solution (1.5 mM) for 15 min [21]. The structure was then thermally oxidized in pure O_2 by a two-step process: pre-oxidation at 400°C for 30 min followed by oxidation at 900°C for 15 min.

2.3. Silicon functionalization

The functionalization procedure was performed on both planar and porous crystalline silicon.

Silicon chip was immersed in freshly prepared Piranha solution (H_2SO_4: H_2O_2 = 4: 1) for 40 min at room temperature, so as to generate –OH functional groups on its surface, extensively washed in milli Q water and dried in a stream of nitrogen gas. The structure was successively silanized in 5% (3-Aminopropyl)triethoxysilane (APTES) in toluene dry solution by immersion at room temperature for 30 min. After silanization, excess of unbound silanes was removed by rinsing sample three times in toluene dry for 2 min. Last step of silanization process was curing on a heater at 100°C for 10 min [22].

Silicon surface was finally functionalized with BS^3 (Bis [sulfosuccinimidyl] suberate), an amino reactive crosslinker. To this aim, 10 mM solution of BS^3 was prepared in 20 mM Hepes buffer pH 7.5. The substrate was covered with this solution at 4°C for 5 h, rinsed twice with deionized water and dried in a stream of nitrogen gas [23].

2.4. Fourier transform infrared spectroscopy (FTIR)

Fourier transform infrared spectroscopy was used to investigate the functionalization procedure performed on PSi surface. FTIR spectra were recorded by a Nicolet Continuµm XL (Thermo Scientific) equipped with a microscope, at 2 cm^{-1} resolution.

2.5. Spectroscopic reflectometry

The reflectivity spectra of the PSi optical structures were acquired by using a simple experimental setup: a white light was sent on the PSi samples by means of a Y optical reflection probe (Avantes). The same probe was used to guide the output signal to an optical spectrum analyzer (Ando AQ6315A). The spectra were acquired at normal incidence over the range 600–1000 nm with a resolution of 0.2 nm.

2.6. Spectroscopic ellipsometry

Ellipsometric measurements on CSi substrate were performed by a Jobin Yvon UVISEL-NIRphase modulated spectroscopic ellipsometer apparatus, at an angle of incidence of 65° over therange 300–1600 nm with a resolution of 5 nm. Thicknesses of films (SiO$_2$, APTES, and BS^3) were measured after each functionalization step.

2.7. Peptide binding

In order to verify the coating and to assess the optimal peptide concentration, BS^3 modified CSi substrates were covered with increasing concentrations (37.5, 75, 150, 300 µM) of labeled peptide and incubated at 4 °C overnight. After incubation, the substrates were washed first with Hepes buffer and then with 1× sodium phosphate buffer (PBS) pH 7.3. Furthermore, substrates were dried in a stream of nitrogen gas. Peptide was labeled with Alexa Fluor 488 C5 Maleimide according to the manufacturer's instructions. Briefly, it was dissolved in Hepes solution (20 mM pH 7.5) at 350 µM final concentration and added to the peptide-modification reagent prepared, under nitrogen flow, mixing a 10-fold molar excess of a reducing agent,

Tris(2-carboxyethyl)phosphine hydrochloride (TCEP), and 1 mM solution of reactive dye in DMSO. The conjugation reaction was allowed for 2 hours at room temperature and in dark conditions. After reaction, labeled peptide was separated from the remaining reactive dye by gel filtration column (Sephadex G-25 column). The labeled peptide concentration was estimated as 80-90% of total peptide amount.

2.8. Fluorescence microscopy

The fluorescence of silicon surfaces functionalized with Alexa Fluor 488 modified-peptide was investigated by means of Leica MZ16 FA fluorescence macroscope equipped with a camera Leica DFC320, by using an optics constituted by a 450–490 nm band-pass excitation filter, a 510 nm dichromatic mirror, and a 515 nm suppression filter. Fluorescence values reported in the work are the average of three different measurements.

2.9. Cell culture

A20 is a murine cell line derived from a spontaneously arising tumor in an aged BALB/c mouse. It pathologically mimics the characteristics of human diffuse large B cell lymphoma [17,24]. The 5T33 murine myeloma cells (5T33MM) were used as control. The cell lines were grown in suspension culture with RPMI 1640 medium (GIBCO, CA, USA), supplemented with 10% fetal bovine serum (GIBCO), 50 units/ml penicillin, 50 μg/ml streptomycin and 2 mM L-glutamine at 37 °C in a 5% CO_2 atmosphere.

2.10. Cells incubation

Label free peptide-modified silicon devices were incubated in presence of 10 μl A20 cells at 5×10^6/mL and 1×10^4/mL concentrations or in the presence of 10 μl 5T33MM cells at 5×10^6/mL in $1 \times$ PBS at 4°C for 2 hours. After incubation, chips were washed three times in $1\times$ PBS and then analyzed under a light microscope. Unless otherwise noted, each measurement was repeated using at least three devices under the same conditions and all observations were carried out at room temperature with a Leica DM6000M microscope (20× objective).

3. Results and discussion

3.1. Chemical functionalization and characterization

The peptide was immobilized on the silicon surface following the functionalization strategy schematized in Fig. 1. This chemical procedure was developed and optimized on PSi sample as a model system because its nanostructured porous peculiar morphology allows the immobilization of a greater number of molecules with respect to a planar substrate and a number of functionalization investigation methods could be more easily exploited [25]. The same optimized procedure was then transferred on CSi sample.

Silanol groups on the oxidized silicon surface were formed by hydroxylation by using aqueous sulfuric acid. APTES in organic anhydrous solvent reacted with silanol groups on the activated surface producing siloxane linkages [26]. The aminosilanized surface was then activated by the homobifunctional crosslinkers BS^3 providing succinimidyl-activated carboxyl group that could react with amine-ended peptide to form an amide bond.
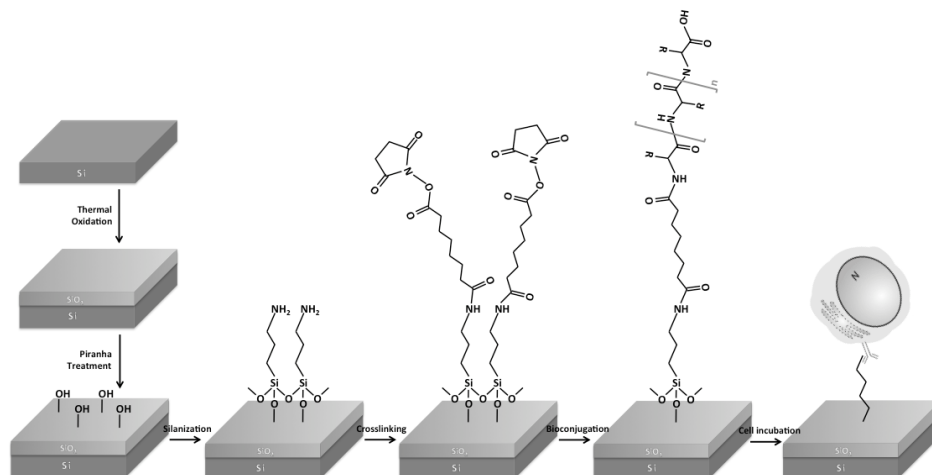
Fig. 1. Scheme of functionalization strategy performed on silicon surface to immobilize a peptide able to specifically detect A20 B lymphoma cells.

Changes in chemical composition of PSi surface were monitored by FTIR spectroscopy after each functionalization step until BS[3] (Fig. 2). The analysis of the FTIR spectra in the range from 2500 to 500 cm^{-1} led to the identification of several characteristic peaks demonstrating the effectiveness of the functionalization procedure. The Si-Hx bonds (at 680-630 cm^{-1} and 2100 cm^{-1}), characteristic of the as-etched PSi, disappeared after the thermal oxidation, and siloxane (Si-O-Si) peak at 1100 cm^{-1} was observed. The APTES silanization was highlighted mainly by the appearance of the characteristic peaks in the range 1440-1390 cm^{-1}, corresponding to CH$_3$ from APTES ethoxy moieties contribution, and the peaks around 1655 cm^{-1}, due to the presence of an imine group produced by the oxidation of an amine bicarbonate salt [26]. Moreover, the formation of a BS[3] layer was confirmed by the presence of the peaks at 1640 and 1550 cm^{-1} corresponding to CO and NH groups of the amide bond respectively.
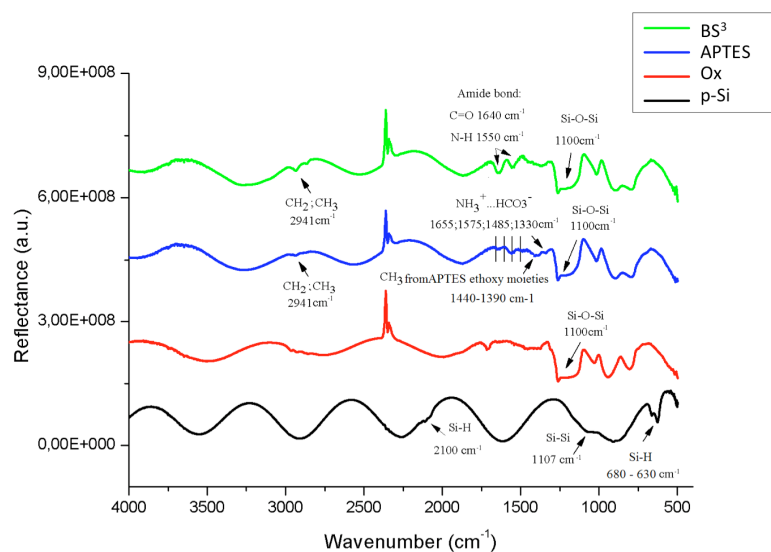

Fig. 2. FTIR spectra of bare PSi (black line), oxidized PSi (red line), oxidized PSi after APTES modification (blue line), oxidized PSi after APTES and BS[3] functionalization (green line).

The functionalization of PSi surface was also confirmed by spectroscopic reflectometry. Figure 3 shows reflectivity spectra of PSi microcavities before (*i.e.*, PSi multilayers thermally oxidized) and after APTES silanization, and after BS[3] functionalization. Red shifts of spectra both for APTES and BS[3] modification were observed. The phenomenon was due to the formation of a thin film of chemical substances on pore walls, which increased the average refractive indices of PSi layers [22]. In particular, a red shift of 21 nm was registered after APTES treatment and of 15 nm after BS[3].
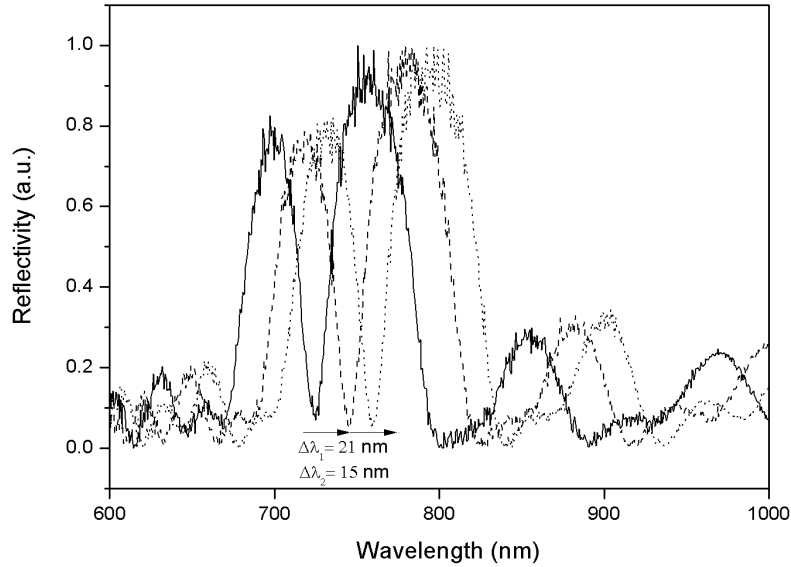

Fig. 3. Reflectivity spectra of PSi microcavity before APTES silanization (solid line), after APTES silanization (dashed line), and after BS[3] functionalization (short dashed line).

Once optimized in terms of reagents and reaction conditions, the functionalization procedure was applied on a planar crystalline silicon support. In this case, each passivation step was monitored by spectroscopic ellipsometry that quantified film thickness changes after thermal oxidation (SiO_2), silanization (APTES), and cross-linker functionalization (BS[3]) for four different samples. Values reported in Table 1 are the average of five determinations on each sample. The thickness of SiO_2 film was 74 ± 1 nm. After reaction with APTES, the thickness increased of 3 nm; a further increase of about 2 nm was observed after the introduction of BS[3].

Table 1. Ellipsometric characterization of film thickness after each reaction step performed on four different samples of crystalline silicon.

Film	Thickness (nm)	Thickness (nm)	Thickness (nm)	Thickness (nm)
	Sample 1	Sample 2	Sample 3	Sample 4
SiO_2	73.5 ± 0.2	74.9 ± 0.3	74.7 ± 0.3	74.9 ± 0.2
APTES	3.1 ± 0.2	3.5 ± 0.2	2.7 ± 0.4	2.9 ± 0.3
BS[3]	1.82 ± 0.03	1.72 ± 0.08	1.78 ± 0.02	1.84 ± 0.03

3.2. Optimization of detection conditions

To investigate the efficiency of the BS[3] modified CSi chip to uniformly bind a peptide on its surface, four increasing concentrations (37.5, 75, 150, 300 μM) of Alexa Fluor 488-labeled peptide (peptide*) were used. Figure 4(a) reports the fluorescence intensities of the CSi biochip surface evaluated by means of a fluorescent macroscope; a dose dependent behavior linear up to 150 μM was observed. Upper image of Fig. 4(b) shows BS[3] modified planar silicon surface after incubation with 150 μM labeled peptide; a high and uniform fluorescence was clearly evident. Upper image of Fig. 4(c) shows instead BS[3] modified porous silicon

surface after incubation with the same concentration of labeled peptide. Also in this case, a similar high and uniform fluorescence was observed. On the contrary, both silicon surfaces functionalized until APTES and incubated with 150 µM labeled peptide as control (lower images 4b and 4c), appeared completely dark.
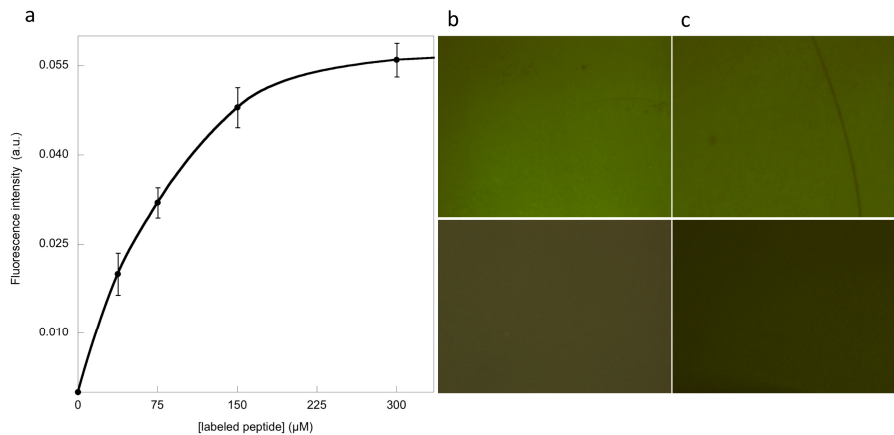

Fig. 4. Binding of fluorescent peptide. (a) Fluorescence intensity of labeled peptide immobilized on silicon chips at different concentrations. (b and c, upper panels) Images of BS[3] modified silicon surface (CSi and PSi, respectively) functionalized with 150 µM labeled peptide compared to silicon functionalized until APTES and treated with 150 µM labeled peptide as control (b and c, lower panels).

3.3. Selective detection of lymphoma cells

Successively, the peptide-functionalized silicon surfaces as chip for label-free detection of cancer cells was exploited.

As experimental model, a murine lymphoma cell line (A20) was chosen. In a previous work, the isolation from random peptide libraries of idiotype peptides that bind specifically the B-cell receptor (BCR) of A20 cells in mice engrafted with A20 lymphoma was reported [17]. Among these peptides, A20-36 peptide (pA20-36) was found the most sensitive and thus suitable for A20 cell detection. The pA20-36 sequence EYVNCDNLVGNCVI was used as target-specific peptide, whereas a random peptide (RND) SSAYGSCKGPCSSGVHSI was used as control.

According to titration results, both peptides were used to bio-functionalize the activated planar and pourous silicon biochip surfaces at 150 µM concentration. Figure 6 shows the A20 cell detection on planar silicon devices. Figure 5(a) shows the microscope light image of the biochip surface after incubation with 100 cells, whereas Fig. 5(b) is related to the incubation with 50,000 cells in order to create saturation-binding conditions. This device was not able to capture A20 cells if functionalized with the RND peptide (Fig. 5(c)), whereas no 5T33MM myeloma cells, a surface IgG-positive B-cell line unable to bind to pA20-36 peptide [17], were observed when incubated on the chip functionalized with pA20-36 (Fig. 5(d)).
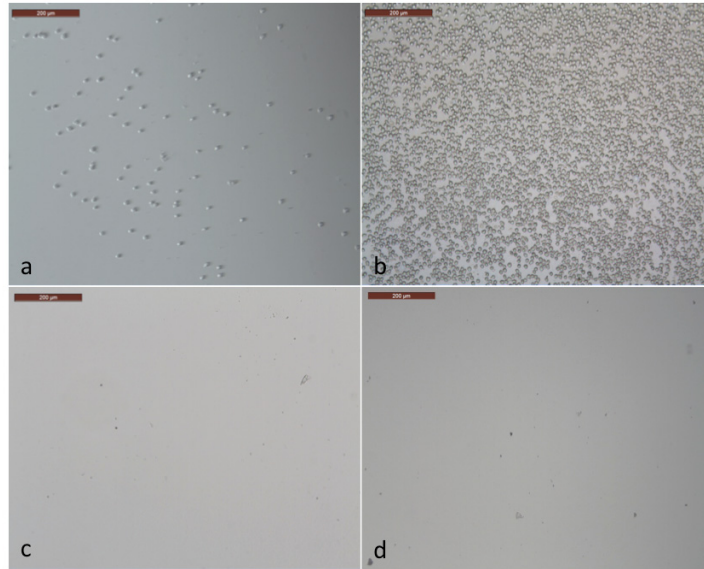
Fig. 5. Representative optical images of A20 cell detection on planar silicon pA20-36 modified-sensor after incubation with 1×10^4 cells/mL (a) and 5×10^6 cells/mL (b). (c) Optical image of RND peptide modified-sensor incubated with A20 cells. (d) Optical image of pA20-36 modified-sensor incubated with 5T33MM cells.

When the A20 cells (50,000) were incubated on A20-36-peptide-functionalized PSi surface a lower number of bound cells was observed on light microscope. Figure 6 shows a comparison between a planar surface biochip (Fig. 6(a)) and a porous surface one (Fig. 6(b)).
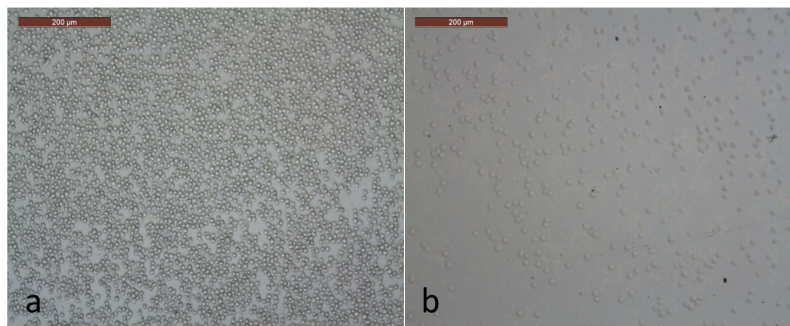

Fig. 6. Representative optical images of A20 cell detection on planar (a) and porous (b) silicon pA20-36 modified-sensor surface after incubation with 5×10^6 cells/mL.

In the same experimental conditions, the number of A20 cells with a unit area of about 80 μm^2 that effectively bind to the functionalized planar surface biochip was by count about 8,500 (~680,000 μm^2). This number was consistent with the available functionalized area (~1.0×10^6 μm^2); whereas, in case of PSi the number of counted cells that bind to the porous surface was about 400 (~32,000 μm^2). The lower number of A20 cells detected by the PSi biochip, compared with the planar surface case, was likely due to its surface morphology. Being highly porous, with pore diameter of about 50 nm, and pore upper edges lower than 1 nm in thickness, the PSi inner surface is many order of magnitude greater than the top active one. Therefore, only an extremely low percentage of the whole number of linked peptides is available on the pore upper edges, and therefore can be seen by the cells (that cannot enter into the pores). Thus, also the number of cells blocked on PSi chip are much less than in the planar surface case.

Defining η as the ratio between the area of the maximum A20 cells layer (~800,000 μm^2) bound on the planar silicon surface and the functionalized available area of the surface (~1.0 × 10^6 μm^2), a theoretical value of η_{th} = 0.8 was calculated. Since the number of counted cells bound on the planar silicon surface was about 8,500 (evaluated by optical microscopy) with a coverage area of ~680,000 μm^2, a value of η_{ex} = 0.68 was calculated. Therefore, the biochip here presented showed a coverage efficiency [(η_{ex}/ η_{th}) × 100] of 85%.

Furthermore, the comparison of the feature of the planar silicon chip based on Id-peptide-BCR recognition with that of an analogous planar silicon chip based on anti-IgG-BCR recognition [8], showed that the first biochip resulted more efficient in detecting A20 cells. In fact, the number of cells detected by the two devices was 8.5 × 10^{-3} cells/μm^2 *vs.* 2.0 × 10^{-3} cells/μm^2, respectively, whereas the difference of coverage efficiency was 65%. This difference could be ascribed to the more easy access of the BCR toward the pA20-36 idiotype peptide with respect to the anti-IgG. As a matter of fact, the binding of IgG to the BCR occurs between the variable region of IgG and the less exposed constant region of BCR, whereas the peptide should bind to the more exposed variable region of BCR. However, a different affinity constant between the two ligand-receptor systems as well as the different functionalization process used might also explain the different detection efficiency observed.

4. Conclusion

Aim of the work was the realization of a highly sensitive silicon-based biochip for lymphoma cells detection. In a previous work [8], we reported the detection of A20 cells by using a silicon platform modified with an IgG antibody as molecular probe directed against B cell receptor. In the present work, a new approach characterized by higher selectivity is presented. It is based on the specificity of an idiotype peptide endowed with high-affinity toward extremely aggressive murine A20 lymphoma cells [24]. The use of a peptide as probe provides a uniform sensor surface coating enhancing capture ability also at low cell concentration. The biochip shows good biocompatibility since neither cell morphology nor viability were affected, and exhibits high repeatability as well as selectivity on label-free cell detection.

The proposed cell detection approach provides a new basis for the development of unique tools for the targeting of patient-specific neoplastic B cells during the minimal residual disease. Indeed, any idiotype peptide is ideally endowed with a unique, clone-specific antigenic reactivity. In this setting, the translation of the Id-peptide approach to patients requires the selection of Id-peptides for each patient through a panning procedure described elsewhere which is time-consuming and expensive [17]. To overcome this major difficulty we are currently focusing on a specific B-cell tumors where a consistent number of patients share the same antigenic reactivity against a restrict pool of Id-peptides.

These results pave the way to the studies of other specific bindings between antibodies and their ligand peptides, allowing to find and characterize new specific receptor-ligand interactions, for instance through the screening of a recombinant phage library.